PHYSICAL REVIEW B **78**, 241402(R) (2008)

Limits of hardness at the nanoscale: Molecular dynamics simulations

Nhon Q. Vo,[1] Robert S. Averback,[1] Pascal Bellon,[1] and Alfredo Caro[2]
[1]*Department of Materials Science and Engineering, University of Illinois, Urbana Champaign, Urbana, Illinois 61801, USA*
[2]*Chemistry, Materials, and Life Sciences Directorate, Lawrence Livermore National Laboratory, Livermore, California 94550, USA*
(Received 10 November 2008; published 29 December 2008)

Contrary to the often reported findings from molecular dynamics computer simulation that metals soften as their grain sizes fall below 10–15 nm, we do not observe such softening in nanocrystalline specimens when they are first thermally relaxed. We offer a simple model that illustrates that the increased hardening is a consequence of grain-boundary relaxation, which suppresses grain-boundary sliding and forces the material to deform by dislocation glide. These observations provide an explanation for why some experiments observe an inverse Hall-Petch relationship at grain sizes below 10–20 nm while others do not.

DOI: 10.1103/PhysRevB.78.241402 PACS number(s): 61.82.Rx, 62.20.F−, 31.15.xv

Materials with grain sizes in the range of a few nanometers often present properties that violate known scaling laws that operate at larger length scales. In particular, hardness, which increases as the grain size of polycrystalline materials decreases, has been predicted to reach exceedingly high values if the grain size could be reduced to the nanoscale.[1] These very hard materials have been indeed found, but departures from the well-known Hall-Petch (H-P) behavior for grain sizes falling below 10–20 nm have prevented them from reaching even higher values of hardness.[2–9] The nature of this departure has been the subject of numerous experimental and computer simulation investigations over the past 20 years. It is now broadly accepted that the validity of the H-P relation must break down as grain dimensions become too small to include dislocation sources. In this new regime, a material's strength becomes controlled by the properties of dislocations created at grain boundaries (GBs) or by other GB processes such as GB sliding; what remains unclear, however, is whether nanocrystalline materials must eventually soften, and if so, at what grain size.

An illuminating approach to studying nanoscale plasticity has been through atomic scale computations. Since the first reports on a change in the mechanism of plasticity,[10,11] computer simulations have consistently shown that the H-P relation breaks down as the grain size decreases, giving way to a regime in which the material softens as the grain size is further decreased. The combination of H-P and the so-called "inverse" H-P behavior gives rise to a maximum in strength at 10–20 nm for all face-centered-cubic metallic materials previously simulated. While many experiments have also reported the existence of inverse H-P behavior, in agreement with the computationally derived picture of plasticity in nanocrystalline materials, they often suffer from difficulties with sample preparation, reproducibility of results, and control of grain size.[12] In fact, experiments now show a diversity of behaviors at small grain sizes, from inverse H-P, to normal H-P, even to a saturation of hardness that is independent of grain size. These studies, like the past computer simulations, have attempted to correlate a material's strength with grain size alone and have not considered the structure of these boundaries. In this Rapid Communication we explore this question by analyzing the effect of thermal annealing on strength at various grain sizes and show that nanoplasticity in annealed samples differs quite substantially from all previous observations using molecular dynamics (MD) simulation. We provide a simple model of nanoplasticity that explains these results, and it helps to place into perspective the results of many past experimental and simulation studies, including a number of newer experimental observations for which the sample microstructures are better defined.[13,14]

The simulations were performed using Cu as a model system, as represented by an embedded atom method (EAM) potential.[15] The molecular dynamics code LAMMPS (Ref. 16) was employed for all simulations. Thermal treatments were performed at zero pressure using Nose-Hoover thermostat and barostat. Contributions to the net strain from the various mechanisms of deformation (elastic, GB sliding, and dislocation glide) were calculated by a local Burgers vector analysis method, which is described elsewhere.[17] The samples in this Rapid Communication were created using a Voronoi polyhedra construction with the samples containing $\approx$1000 grains for samples with an average grain size of 2.5 nm, 150 grains for samples with 4 and 5 nm grain size, and 46 grains for samples with 10–20 nm grain size; no differences were observed using different initial configurations of the samples. After being relaxed at 300 K for 20 ps to stabilize the structure, the samples were annealed at elevated temperatures for times up to 2.5 ns at zero external pressure. After annealing, the samples were cooled back to room temperature over a 10 ps interval. Three sets of samples were thus created. The first set, or as-prepared samples, was relaxed at 300 K for 20 ps. The second set was relaxed at 1000 K for 750 ps; only negligible grain growth was observed in these samples, as shown in Fig. 1(a). The last set of samples had initial grain sizes of $\approx$2.5 nm but which had undergone grain growth during the high-temperature annealing (at 1000 K up to 1200 ps and at 1200 K for an additional 1200 ps); see inset of Fig. 1(a). Uniaxial compression tests at 300 K for strains up to $\varepsilon=0.2$ were performed on all samples, using deformation rates of 1×10^{10} and 1×10^{9} s^{-1}, on all samples.

Figure 1(a) shows the time evolution of the average grain size during the annealing process for all samples. Twins were observed to form during the annealing; they are counted as separate grains, in accordance with recent models of polycrystalline plasticity.[18] Only the sample with a 2.5 nm initial grain size shows significant grain growth; the small decrease in grain size in the 10 and 15 nm samples is due to twin formation. While little grain growth is observed in most

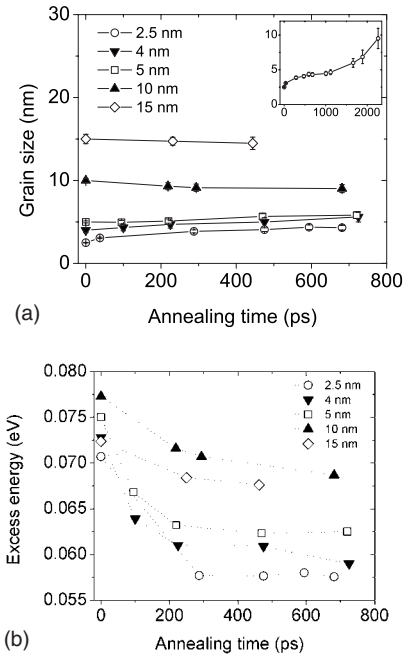

FIG. 1. (a) Evolution of the grain size and (b) excess GB energy/atom versus annealing time at $T=1000$ K for different grain sizes. The 2.5 nm sample was annealed at 1200 K after 1200 ps. (See inset.)

samples, the average excess energy of atoms located on grain boundaries decreases for all samples as shown in Fig. 1(b). Atoms on twin boundaries are not included in this average.

Shown inset in Fig. 2 are stress-strain curves for samples with ≈5 nm grain size: the as-prepared sample and the one annealed for 720 ps. These curves illustrate that annealed samples are harder than as-prepared samples of corresponding grain size. Note that in the early stages of deformation all samples show the same elastic response but that the yield and flow stresses increase substantially upon annealing. In a similar vein, Hasnaoui *et al.*[19] observed less total strain in annealed than in unannealed samples with 12 nm grain size in simulations performed at constant load.

A key to understanding this behavior is provided by ex-

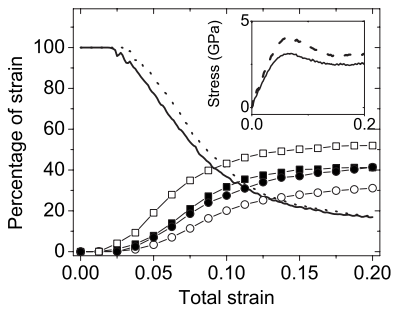

FIG. 2. Contributions to strain from different mechanisms for as-prepared and annealed samples with 5 nm grain size: elastic (lines), GB sliding (squares), and dislocation glide (circles). As-prepared sample represented by open symbols, solid line, and sample annealed for 720 ps by solid symbols and dotted line. The inset shows stress-strain behavior of 5 nm samples as-prepared (solid line) and after annealing for 720 ps (dashed line).

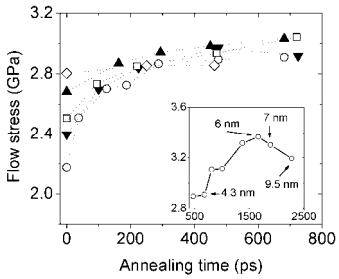

FIG. 3. Flow stress as a function of annealing time at 1000 K for samples of different grain size: 2.5 nm (○), 4 nm (▼), 5 nm (□), 10 nm (▲), and 15 nm (◇). The inset shows the flow stress of the 2.5 nm sample versus annealing time (at 1200 K after 1200 ps). The grain size of this sample is indicated at various annealing times.

amining the relative contributions of dislocation glide, GB sliding, and elastic deformation to the total deformation. The main portion of Fig. 2 shows the results for the two samples reported in the inset. The as-prepared sample, which has larger GB energies, as shown in Fig. 1(b), begins to deform plastically by GB sliding. At strains above $\varepsilon \sim 0.12$, the GB sliding contribution saturates at ~50%. Dislocation glide, on the other hand, initiates much later than GB sliding ($\varepsilon > 0.05$), and it then rises slowly before reaching a contribution of 30% at $\varepsilon=0.2$. GB sliding therefore provides the larger contribution to plastic strain in as-prepared samples and particularly so at small strains. The deformation behavior is quite different in the annealed samples: the GB sliding contribution to deformation is significantly smaller; it appears later in the strain response ($\varepsilon \sim 0.05$); it is half of its value in the as-prepared sample over the range of $0.05 < \varepsilon < 0.10$, and it saturates at ≈40% at $\varepsilon=0.2$. Notably, the contribution from dislocation glide is nearly the same as that due to GB sliding even at small strains.

The nearly identical contributions of GB sliding and dislocation glide in the annealed sample suggest that GB sliding in annealed samples might simply be a part of the dislocation accommodation process, which is necessary for dislocation creation and annihilation at the GBs and the associated grain rotation. We will show later that this conjecture is consistent with data obtained at all grain sizes.

Figure 3 shows the dependence of flow stress on annealing time for all samples; again we point out that grain growth was negligible in all samples during these annealing times. Flow stresses in these various samples increase from their initial values and converge to a single value. Similar behavior is observed for the yield stress (not shown). The increase in flow stress with grain size seen prior to annealing, $t=0$, or inverse H-P behavior is thus no longer observed after annealing, with the flow stresses becoming independent of grain size. The inset of Fig. 3, on the other hand, shows that the flow stress of the 2.5 nm sample continues to increase during more extensive annealing when grain growth becomes significant (see Fig. 1). This sample reaches flow stresses ≈10% higher than those observed in Fig. 3, reaching a maximum when the grain size is ≈6 nm.

Figure 4 shows the integral percentages of plastic strain deriving from GB sliding and dislocation glide measured at

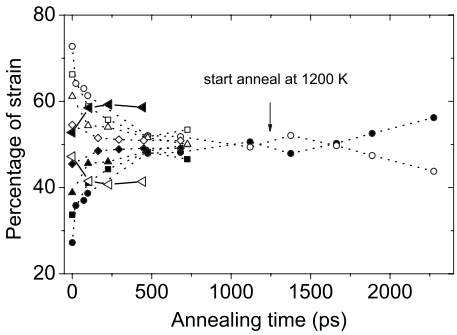

FIG. 4. Percentage of contribution to plastic deformation from dislocations (solid symbols) and GB sliding (open symbols) versus annealing time prior to deformation for (●) 2.5 nm, (■) 4 nm, (▲) 5 nm, (◆) 10 nm, and (◀) 15 nm grain sizes.

$\varepsilon=0.20$ as a function of annealing time. As expected from the above and previous work,[17] dislocation glide in the as-prepared samples is an increasing function of grain size (33% for 4 nm, 36% for 5 nm, 46% for 10 nm, and 53% for 15 nm). As the annealing time reaches ~400 ps, however, the contributions of these two mechanisms become equal and, notably, independent of grain size below ≈10 nm. This observation supports our conjecture above that GB sliding in these annealed samples is linked to the dislocation activity.

These various findings are collected in a H-P diagram of flow stress versus grain size in Fig. 5. We notice, first of all, a wide range of behaviors: inverse H-P behavior is observed in the unannealed sample; a plateau in the flow stress for grain sizes below ≈10 nm in samples annealed for 750 ps; and an extension of the H-P relation to ≈6 nm in the more extensively annealed 2.5 nm sample. Below this grain size the sample behaves similarly to the as-prepared samples, presumably because twinning and grain-boundary relaxation are not yet complete.

These results, which show a strong sensitivity of hardness to the nature of the GB structure, help to address the fundamental issues of whether an intrinsic hardness can meaningfully be assigned to nanocrystalline materials and which algorithm of numerical synthesis is best suited to represent experimental conditions. We consider, for example, the combined results of Figs. 4 and 5. In the regime that the hardness

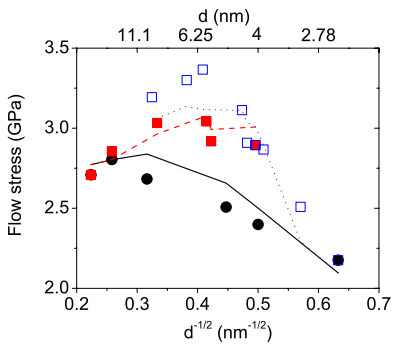

FIG. 5. (Color online) Flow stress as a function of grain size of set 1, as-prepared (●), set 2, annealed (■), and set 3, 2.5 nm samples annealed to larger grain sizes (□). The strain rate is 1×10^{10} s^{-1}.

is independent of grain size, the fraction of strain due to dislocation glide equals that due to GB sliding. As the grain size becomes larger, normal H-P behavior is observed and the contribution due to dislocation glide increases. In the as-prepared samples, the inverse H-P relation is observed and the contribution of strain due to GB sliding increases above that due to dislocations. The hardness of a sample thus depends on the ratio of GB sliding to dislocation glide, as well as to the exact size of the grains. In an attempt to quantify this behavior, we express the flow stress in terms of GB sliding and dislocation glide contributions. At large grain sizes, the flow stress is determined by dislocation glide, while for very small grain sizes with unrelaxed boundaries, the flow stress is determined by GB sliding. We thus write the flow stress in the form

$$\frac{1}{\sigma}=\frac{1}{k_1+\dfrac{k_2}{d^{1/2}}}\left(1-\frac{N_{\mathrm{GB}}}{N_{\mathrm{tot}}}\right)+k_3(E_{\mathrm{GB}})\left(\frac{N_{\mathrm{GB}}}{N_{\mathrm{tot}}}\right), \tag{1a}$$

where N_{GB} is the total number of atoms in GBs and N_{tot} is the number of atoms in the computational cell, k_1 and k_2 are constants, and k_3 is a parameter depending on the GB energy, E_{GB}. Since $N_{\mathrm{GB}}/N_{\mathrm{tot}}$ varies as $1/d$, Eq. (1a) provides the correct limiting cases; i.e., at large grain sizes the H-P relation is recovered, while at small grain sizes the flow stress results from GB sliding, varying linearly with d as observed in Ref. 10. A similar form for the flow stress can be obtained by using the rule of mixtures and assuming that grain interiors and GBs represent separate phases that are arranged in parallel.[8] Our simulations illustrate that the parameter k_3 is dependent upon the degree of GB relaxation. Since the predominant effect of annealing is to reduce the number of high-energy boundaries and replace them with twin boundaries, we approximate Eq. (1a) by assuming that twin boundaries are completely relaxed and do not contribute to sliding. Any additional changes due to the relaxation of high-energy boundaries during annealing are assumed to be smaller and accounted for, in part, by a reduced value of N_{GB}. We therefore assume $k_3=k_3'$ is a constant and rewrite Eq. (1a) in the form

$$\frac{1}{\sigma}=\frac{1}{k_1+\dfrac{k_2}{d^{1/2}}}\left(1-\frac{N_{\mathrm{GB}}-N_{\mathrm{twin}}}{N_{\mathrm{tot}}}\right)+k_3'\left(\frac{N_{\mathrm{GB}}-N_{\mathrm{twin}}}{N_{\mathrm{tot}}}\right). \tag{1b}$$

The values of σ, N_{GB}, and N_{twin} can be found directly from the simulations for the three sets of samples, and these values were used to determine the three constants, k_i, in Eq. (1b). The results of this model are shown in Fig. 5 for a strain rate of 1×10^{10} s^{-1}. Results at 1×10^{9} s^{-1} (not shown) are similar. The dashed lines represent fits to Eq. (1b), with a single set of constants for each strain rate (a) 1×10^{10} s^{-1} ($k_1=1.55$ GPa, $k_2=6.29$ GPa $nm^{1/2}$, and $k_3=0.55$ GPa^{-1}), and (b) 1×10^{9} s^{-1} ($k_1=1.55$ GPa, $k_2=3.8$ GPa $nm^{1/2}$, and $k_3=0.74$ GPa^{-1}). These plots thus illustrate that a simple plot of flow stress versus grain size, without regard to the state of grain-boundary relaxation, has no intrinsic value. On the

other hand, they show that all of the data can be reasonably fit by a simple model of plasticity that includes grain-boundary relaxation. Lastly, it can be seen for the case of as-prepared samples, i.e., unrelaxed grain boundaries, that the first term in Eq. (1b) dominates for $d \geq 15-20$ nm, which is in excellent agreement with previous MD simulations.[10,11] We verified, in fact, that Eq. (1b) fits well to the simulation data in Ref. 10 if we assume that $N_{\text{twin}}=0$ for their unannealed specimens. The constants differ somewhat, however, owing to the different strain rate employed and the wider range of grain sizes.

These observations provide a perspective for viewing the broad spectrum of experimental results on nanoscale plasticity. First, many of the earlier experiments cited above showed inverse H-P behavior as the grain sizes were reduced below 10–20 nm. These samples were often produced by compaction of nanopowders, followed by thermal annealing to increase the grain size. This behavior is thus quite similar to that observed in our simulation samples comprising set 3 samples, i.e., initially 2.5 nm. The maximum in the hardness occurs at ≈ 6 nm in the simulation, which is below that found in the experiments, but this is probably a consequence of our strain rates being several orders of magnitude larger than the experiments and also because our initial grain size was 2.5 nm compared to the 5–10 nm typical of these experiments. Our results also bear a remarkable similarity to several more recent experimental reports. Trelewicz and Schuh[13] succeeded in preparing a set of Ni-W alloy samples with grain sizes between 3 and 150 nm using pulsed electrodeposition. They observed that as grain size decreases, plasticity shifts from crystal-like behavior (Hall-Petch) to amorphous or glassylike behavior, where hardness is independent of grain size. Their results are very similar to our sample set 2, as shown in Fig. 5. Wang *et al.*,[14] moreover, studied the effect of thermal annealing on electrodeposited nanocrystalline Ni and found the unexpected result that strength first increases rather than decreases upon annealing at low temperatures. They concluded that at the low annealing temperatures employed, grain-boundary relaxation was sufficient to strengthen the material, but that impurity segregation and grain growth could be suppressed. These results and conclusions agree well with our simulations.

In summary, this work shows that by relaxing the grain boundaries by a brief high-temperature annealing treatment, the strength of nanocrystalline materials can be greatly modified. In particular, plasticity in unrelaxed samples shows a transition from normal Hall-Petch behavior for grain sizes above ≈ 12 nm to inverse Hall-Petch; in partially relaxed samples, a regime below 12 nm is observed where the strength becomes independent of grain size; and in samples undergoing grain growth during relaxation, H-P behavior extends to significantly smaller grain sizes. Our analysis linking the relationship between GB sliding and GB relaxation offers a key to resolving the long-standing controversy concerning the inverse H-P relation, as it illustrates that grain size alone is not sufficient to characterize hardness in nanoscale systems but that a measure of GB relaxation is required as well.

This work was supported by the U.S. Department of Energy, Basic Energy Sciences under Grant No. DEFG02-05ER46217, the DOE National Nuclear Security Administration under Grant No. DEFG52-06NA26153, and in part under the auspices of the U.S. Department of Energy by Lawrence Livermore National Laboratory under Contract No. DE-AC52-07NA27344.

[1] A. H. Chokshi, A. Rosen, J. Karch, and H. Gleiter, Scr. Metall. **23**, 1679 (1989).
[2] M. Dao, L. Lu, R. J. Asaro, J. T. M. De Hosson, and E. Ma, Acta Mater. **55**, 4041 (2007).
[3] H. Gleiter, Acta Mater. **48**, 1 (2000).
[4] S. R. Agnew, B. R. Elliott, C. J. Youngdahl, K. J. Hemker, and J. R. Weertman, Mater. Sci. Eng., A **285**, 391 (2000).
[5] C. C. Koch, Scr. Mater. **49**, 657 (2003).
[6] S. Cheng, J. A. Spencer, and W. W. Milligan, Acta Mater. **51**, 4505 (2003).
[7] D. Wolf, V. Yamakov, S. R. Phillpot, A. Mukherjee, and H. Gleiter, Acta Mater. **53**, 1 (2005).
[8] M. A. Meyers, A. Mishra, and D. J. Benson, Prog. Mater. Sci. **51**, 427 (2006).
[9] K. S. Kumar, H. Van Swygenhoven, and S. Suresh, Acta Mater. **51**, 5743 (2003).
[10] J. Schiøtz, F. D. DiTolla, and K. W. Jacobsen, Nature (London) **391**, 561 (1998); J. Schiøtz and K. W. Jacobsen, Science **301**, 1357 (2003).
[11] H. Van Swygenhoven and A. Caro, Nanostruct. Mater. **9**, 669 (1997); H. Van Swygenhoven, M. Spaczer, A. Caro, and D. Farkas, Phys. Rev. B **60**, 22 (1999).
[12] C. C. Koch and J. Narayan, in *Structure and Mechanical Properties of Nanophase Materials—Theory and Computer Simulations vs Experiment*, MRS Symposia Proceedings No. 634 (Materials Research Society, Pittsburgh, PA, 2000), p. B5.1.
[13] J. R. Trelewicz and C. A. Schuh, Acta Mater. **55**, 5948 (2007).
[14] Y. M. Wang, S. Cheng, Q. M. Wei, E. Ma, T. G. Nieh, and A. Hamza, Scr. Mater. **51**, 1023 (2004).
[15] M. R. Sorensen, Y. Mishin, and A. F. Voter, Phys. Rev. B **62**, 3658 (2000).
[16] S. Plimpton, J. Comput. Phys. **117**, 1 (1995).
[17] N. Q. Vo, R. S. Averback, P. Bellon, S. Odunuga, and A. Caro, Phys. Rev. B **77**, 134108 (2008).
[18] G. Proust, C. N. Tomé, and G. C. Kaschner, Acta Mater. **55**, 2137 (2007).
[19] A. Hasnaoui, H. Van Swygenhoven, and P. M. Derlet, Acta Mater. **50**, 3927 (2002).